

The importance of dry and wet merging on the formation and evolution of elliptical galaxies

L. Ciotti¹, B. Lanzoni², M. Volonteri³

¹ *Dipartimento di Astronomia, Università di Bologna, via Ranzani 1, 40127 Bologna, Italy*

² *INAF – Osservatorio Astronomico di Bologna, via Ranzani 1, 40127, Bologna, Italy*

³ *Institute of Astronomy, University of Cambridge, Madingley Road, UK*

November 10, 2006, accepted version

ABSTRACT

With the aid of a simple yet robust approach we investigate the influence of dissipationless and dissipative merging on galaxy structure, and the consequent effects on the scaling laws followed by elliptical galaxies. Our results suggest that ellipticals cannot be originated by parabolic merging of low mass spheroids only, even in presence of substantial gas dissipation. However, we also found that scaling laws such as the Faber-Jackson, Kormendy, Fundamental Plane, and the $M_{BH} - \sigma$ relations, when considered over the whole mass range spanned by ellipticals in the local universe, are robust against merging. We conclude that galaxy scaling laws, possibly established at high redshift by the fast collapse in pre-existing dark matter halos of gas rich and clumpy stellar distributions, are compatible with a (small) number of galaxy mergers at lower redshift.

Subject headings: galaxies: elliptical and lenticulars, cD – galaxies: evolution – galaxies: formation – galaxies: structure – galaxies: fundamental parameters

1. Introduction

Early-type galaxies are known to follow well defined empirical scaling laws relating their global observational properties, such as total luminosity L , effective radius R_e , and central velocity dispersion σ . Among others we recall the Faber & Jackson (1976, hereafter FJ), Kormendy (1977), Fundamental Plane (Djorgovski & Davis 1987; Dressler et al. 1987; hereafter FP), the color- σ (Bower, Lucey & Ellis 1992), and the $M_{g2} - \sigma$ (e.g., Guzman et al. 1992; Bernardi et al. 2003c) relations. In addition, it is now believed that all elliptical galaxies host a central supermassive black hole (SMBH; e.g., see de Zeeuw 2001), whose mass

M_{BH} scales with the stellar mass M_* and velocity dispersion σ of the host galaxy (Magorrian et al. 1998; Ferrarese & Merritt 2000; Gebhardt et al. 2000; Tremaine et al. 2002). Clearly, these scaling relations provide invaluable information about the formation and evolution of early-type galaxies, and set stringent constraints to galaxy formation models.

The two major formation models for ellipticals that have been proposed so far are the monolithic (Eggen, Lynden-Bell & Sandage 1962), and the merging (Toomre 1977; White & Frenk 1991) scenarios. Each of them scores observational and theoretical successes and drawbacks (e.g., see Ostriker 1980, Renzini 2006). For instance, we list here three observational and theoretical evidences in favour of a fast and dissipative monolithic-like collapse.

First, the observed color-magnitude and Mg_2 - σ relations, and the increase of the $[\alpha/Fe]$ ratio with σ in the stellar population of elliptical galaxies (e.g., see Jørgensen 1999, Thomas, Greggio & Bender 1999 Saglia et al. 2000; Bernardi et al. 2003c, and references therein), suggest that star formation in massive ellipticals was not only more efficient than in low mass galaxies, but also that it was a faster process (i.e., completed before SNIa explosions take place), with the time scales of gas consumption and ejection shorter or comparable to the galaxy dynamical time (e.g., see Matteucci 1994, Pipino & Matteucci 2004), and decreasing for increasing galaxy mass.

Second, structural and dynamical properties of ellipticals are well reproduced by cold dissipationless collapse, a process which is expected to dominate the last stages of highly dissipative collapses, in which the gas cooling time of the forming galaxy is shorter than its dynamical time, so that stars form ‘in flight’, and the subsequent dynamical evolution is a dissipationless collapse. It is now well established that the end-products of cold and phase-space clumpy collapses have projected density profiles well described by the $R^{1/4}$ de Vaucouleurs (1948) law, radially decreasing line-of-sight velocity dispersion profiles, and radially increasing velocity anisotropy, in agreement with what observed in elliptical galaxies (e.g., see van Albada 1982; May & van Albada 1984; McGlynn 1984; Aguilar & Merritt 1990; Londrillo, Messina & Stiavelli 1991; Udry 1993; Hozumi, Burkert, & Fujiwara 2000; Trenti, Bertin & van Albada 2005).

Third, the current and remarkably succesful cosmological scenario for structure formation predicts that well defined scaling laws are imprinted in the dark matter halos; in particular, the virial velocity dispersion of DM halos increases as $\sigma_v \propto M_{DM}^{1/3}$. This because virialized DM halos are the *collapse* end-products of negative energy (inhomogeneous) density distributions, in which the absolute value of the binding energy per unit mass increases with the halo mass (Peebles 1980). On the contrary, in a parabolic merging σ_v would not increase with halo mass.

Thus the observed scaling laws of elliptical galaxies could be originated by the fast collapse of inhomogeneous gas and star distributions in pre-existing DM halos, rather than by parabolic merging processes (e.g., see Lanzoni et al. 2004). Note that high resolution N-body simulations (Nipoti, Londrillo & Ciotti 2006) have shown that cold (dissipationless) collapses in pre-existing DM halos nicely reproduce the weak homology of elliptical galaxies (e.g., see Caon, Capaccioli & D’Onofrio 1993; Prugniel & Simien 1997; Bertin, Ciotti & Del Principe 2002, hereafter BCD02; Graham & Guzmán 2003) and the central break radius in their surface brightness profile (Ferrarese et al. 1994; Lauer et al. 1995; Graham et al. 2003; Trujillo et al. 2004).

The last point above is particularly puzzling because the available observations seem to indicate that mergers may happen in the life of elliptical galaxies, with dissipative (wet) mergers dominating at high redshift, and gas-free (dry) merging mainly affecting massive ellipticals at $z \lesssim 1.5$ (e.g., see Bell et al. 2004, 2006; van Dokkum 2005; Faber et al. 2005; Conselice 2006). This picture is also suggested by the available information on the star formation history of the Universe and the redshift evolution of the quasar luminosity function (see, e.g., Haehnelt & Kauffmann 2000; Burkert & Silk 2001; Yu & Tremaine 2002; Cavaliere & Vittorini 2002; Haiman, Ciotti & Ostriker 2004). In addition, parabolic orbits seem to be quite relevant in the hierarchical merging picture (e.g., see Benson 2005; Khochfar & Burkert 2006). To get insights on this issue, in the present paper we will focus on the remarkable homogeneity and regularity of the family of early-type galaxies (testified by their scaling laws), and we explore the consequences of galaxy merging on them.

The impact of dry merging on the scaling laws of early-type galaxies has been already investigated in several works (e.g., Capelato, de Carvalho & Carlberg 1995; Pentericci, Ciotti & Renzini 1996; Haehnelt & Kauffmann 2000; Ciotti & van Albada 2001, hereafter CvA01; Evstigneeva, Reshetnikov & Sotnikova 2002; Nipoti, Londrillo & Ciotti 2003, hereafter NLC03; González-García & van Albada 2003; Dantas et al. 2003; Evstigneeva et al. 2004; Boylan-Kolchin, Ma & Quataert 2005, 2006). In particular, the simple approach of CvA01 and the N-body simulations of NLC03 showed that repeated, parabolic merging of gas-free galaxies is unable at reproducing the observed scaling laws, because the merger-products are characterized by unrealistically large effective radius and mass-independent velocity dispersion (see also Shen et al. 2003). However, simple physical arguments show that gas dissipation should be able to mitigate the problems posed by dry merging to the explanation of the observed scaling laws (e.g., see CvA01; Kazantzidis et al. 2006; Robertson et al. 2006ab; Dekel & Cox 2006)¹. Unfortunately, numerical simulations with gas

¹Note that by comparing the FP of galaxies and that of galaxy clusters, Burstein et al. (1997) and Lanzoni et al. (2004) suggested that, at variance with groups and clusters, gas dissipation must have had

dissipation are considerably more complicate than pure N-body simulations (e.g., see Sáiz, Domínguez-Tenreiro & Serna 2004; Oñorbe et al. 2005, 2006; Robertson et al. 2006ab), and, in particular, very few of them have been done from realistic cosmological initial conditions (e.g., see Naab et al. 2006, and references therein). For these reasons, by generalizing the approach presented in CvA01 to the dissipative case, we further investigate with Monte-Carlo simulations the compatibility of galaxy merging with the formation and evolution of early-type galaxies, focusing in particular on 1) the effects of gas dissipation on the merger end-products (wet merging), and 2) the effects of parabolic dry and wet merging on the scaling laws followed by elliptical galaxies in the local universe. We argue that parabolic merging of low-mass seed galaxies alone cannot be at the origin of the scaling laws, even though wet mergers lead to early-type galaxies following the observed scaling laws better than the end products of dry merging. We also show that galaxy scaling laws, such as the FJ, Kormendy and FP relations, once in place, are robust against merging. Thus, our results reinforce the idea that monolithic-like collapse at early times and subsequent merging could just represent the different phases of galaxy formation (collapse) and evolution (merging, in addition to the aging of the stellar populations and related phenomena).

The paper is organized as follows. In Section 2 we derive the recursive equations describing the evolution of galaxy properties after dry and wet parabolic mergers, and in Section 3 we discuss in detail the case of equal-mass merging. In Section 3 we use the derived relations in Monte-Carlo investigations of merging of elliptical galaxy populations, and the main results are finally summarized and discussed in Section 4.

2. The models

In this Section we now derive from elementary physics arguments the relations between the properties of the progenitor galaxies and those of the merging end-products that will be used in the rest of the paper. For simplicity in the adopted scheme each elliptical is modeled as a non rotating, isotropic and spherically symmetric virialized system, characterized by a stellar mass M_* , a gas mass $M_g = \alpha M_*$, and a SMBH mass $M_{BH} = \mu M_*$; from observations $\mu \simeq 10^{-3}$ in $z = 0$ spheroids (Magorrian 1998). In our treatment we do not consider the presence of a DM halo, as it could be introduced just by rescaling the model stellar mass-to-light ratio if the DM density distribution is proportional to the stellar one, as discussed in the following paragraphs. The total energy of a galaxy is then given by

$$E = K_* + U_g + W, \tag{1}$$

an important role on the formation and evolution of ellipticals.

where

$$K_* = \frac{3}{2} \int \rho_* \sigma_*^2 dV \quad (2)$$

is the stellar kinetic energy, and

$$U_g = \frac{3 k_B}{2 \langle m \rangle} \int \rho_g T dV \quad (3)$$

is the gas internal energy; σ_* , k_B , T , and $\langle m \rangle$ are the stellar 1-dimensional velocity dispersion, the Boltzmann constant, the gas temperature, and the gas mean molecular mass, respectively. Finally

$$W = \frac{1}{2} \int (\rho_* + \rho_g)(\phi_* + \phi_g) dV \quad (4)$$

is the total gravitational energy of stars and gas (we do not consider the negligible contribution of the central SMBH).

Under the simplifying assumption that the gas is spatially distributed as the stars (i.e., $\rho_g = \alpha \rho_*$), then $\phi_g = \alpha \phi_*$, and

$$W = (1 + \alpha)^2 W_*, \quad (5)$$

where W_* is the self-gravitational energy of the stellar component. Furthermore, assuming that the gas is in equilibrium in the total gravitational field, from the Jeans and the hydrostatic equations it results that $T = \langle m \rangle \sigma_*^2 / k_B$, and from equations (2)-(3)

$$U_g = \alpha K_*. \quad (6)$$

Finally, from equations (5)-(6) and the virial theorem for the two-component system of stars + gas, the total galactic energy can be written in terms of the stellar energy and of the relative amount of gas as

$$E = -(1 + \alpha) K_* = \frac{(1 + \alpha)^2}{2} W_*. \quad (7)$$

Note that a DM halo of mass $M_{\text{DM}} = \alpha_{\text{DM}} M_*$ distributed as the stars would be easily considered in the present scheme by the addition of the new parameter α_{DM} in equations (5)-(7).

The quantities introduced so far are not directly observables, and so in Section 2.1 we will show how to relate the characteristic one-dimensional stellar velocity dispersion σ_v and the characteristic radius r_v , defined as

$$K_* \equiv \frac{3}{2} M_* \sigma_v^2, \quad (8)$$

$$|W_*| \equiv \frac{G M_*^2}{r_v}, \quad (9)$$

to the galaxy effective radius R_e and central projected velocity dispersion σ^2 .

We now focus on the parabolic merging of two galaxies, so that the total energy of the system is the sum of the internal potential and kinetic energies of the two progenitor galaxies; we also assume that no mass is lost in the process. During the merging, as a consequence of gas dissipation, a fraction η of the available gas mass is converted into stars, and the stellar mass balance equation is

$$M_* = M_{*1} + M_{*2} + \eta(M_{g1} + M_{g2}). \quad (10)$$

Furthermore, a new SMBH forms by the coalescence of the two central BHs and a fraction $f\eta$ of the available gas is accreted on it, leading to a BH of final mass

$$M_{BH} = (M_{BH1}^p + M_{BH2}^p)^{1/p} + f\eta(M_{g1} + M_{g2}). \quad (11)$$

The free parameter $1 \leq p \leq 2$ describes how much BH rest mass is radiated as gravitational waves during the BH coalescence: $p = 1$ corresponds to the classical merging case (no gravitational radiation), while $p = 2$ to the maximally radiative case for non-rotating BHs. Note that in equation (11) it is implicitly assumed that first M_{BH1} and M_{BH2} merge, and then the gas is accreted on the new BH; the other extreme case would be that of gas accretion followed by merging (e.g., see Hughes & Blandford 2003). Of course, if $p = 1$ there is no difference in the final mass; we anticipate that in the Monte-Carlo simulations described in Section 3 we explored both cases, finding not significant differences. As a consequence of star formation and BH accretion, the gas mass balance equation is

$$M_g = (1 - \eta - f\eta)(M_{g1} + M_{g2}), \quad (12)$$

which implies that $0 \leq \eta \leq 1/(1 + f)$. Thus, the gas-to-star mass ratio after the merger and the new Magorrian coefficient are given by

$$\alpha \equiv \frac{M_g}{M_*} = \frac{(1 - \eta - f\eta)(\alpha_1 M_{*1} + \alpha_2 M_{*2})}{(1 + \eta\alpha_1)M_{*1} + (1 + \eta\alpha_2)M_{*2}}, \quad (13)$$

while

$$\mu \equiv \frac{M_{BH}}{M_*} = \frac{(\mu_1^p M_{*1}^p + \mu_2^p M_{*2}^p)^{1/p} + f\eta(\alpha_1 M_{*1} + \alpha_2 M_{*2})}{(1 + \eta\alpha_1)M_{*1} + (1 + \eta\alpha_2)M_{*2}}, \quad (14)$$

²Note that σ_v and r_v in equations (8) and (9) coincide with the virial velocity dispersion and the virial radius of the star+gas system. This would not be true in a system where $\rho_* \neq \rho_g$.

respectively. Note that if $p = 1$ and $f = \mu_1 = \mu_2$, the proportionality coefficient μ remains unchanged after the merging; also note that the scheme above is generalizable by allowing for different values of f and η in the two progenitor galaxies, but for simplicity in this paper we assume f and η fixed.

In order to describe the effects on r_v and σ_v of the radiative energy losses associated with gas dissipation, a fraction $(1 + f)\eta$ of the gas internal energy U_g of each progenitor is subtracted from the total energy budget of the merger-product, consistently with the previous assumptions³. Thus, from equation (6), the final total energy of the remnant is

$$E = E_1 + E_2 - \eta(1 + f)(\alpha_1 K_{*1} + \alpha_2 K_{*2}). \quad (15)$$

Identity (7) with the new total energy E , the new mass ratio α and the new total stellar mass M_* are given by equations (15), (13), and (10), respectively. Simple algebra shows that for the new galaxy

$$\sigma_v^2 = \frac{M_{*1} + M_{g1}}{M_* + M_g} A_1 \sigma_{v1}^2 + \frac{M_{*2} + M_{g2}}{M_* + M_g} A_2 \sigma_{v2}^2, \quad (16)$$

and

$$\frac{1}{r_v} = \left(\frac{M_{*1} + M_{g1}}{M_* + M_g} \right)^2 \frac{A_1}{r_{v1}} + \left(\frac{M_{*2} + M_{g2}}{M_* + M_g} \right)^2 \frac{A_2}{r_{v2}}, \quad (17)$$

where

$$A_1 = 1 + \frac{(1 + f)\eta\alpha_1}{1 + \alpha_1}, \quad (18)$$

and a similar expression holds for A_2 . In a dry ($\eta = 0$) merging $A_1 = A_2 = 1$, so that

$$\min(\sigma_{v1}^2, \sigma_{v2}^2) \leq \sigma_v^2 = \frac{(1 + \alpha_1)M_{*1}\sigma_{v1}^2 + (1 + \alpha_2)M_{*2}\sigma_{v2}^2}{(1 + \alpha_1)M_{*1} + (1 + \alpha_2)M_{*2}} \leq \max(\sigma_{v1}^2, \sigma_{v2}^2), \quad (19)$$

i.e., the virial velocity dispersion of the merger-product cannot be larger than the maximum velocity dispersion of the progenitors (the $\alpha > 0$ and $\eta = 0$ case also describes the situation in which the gaseous component is replaced by a DM halo). Instead, $A > 1$ in case of wet ($\eta > 0$) merging, and the resulting σ_v is larger than in the dry case, possibly larger than the maximum velocity dispersion of the progenitors. A similar argument shows that in presence of gas dissipation the new r_v increases less than in the dry case. Note that the conclusions of this preparatory analysis are obtained under the hypothesis of parabolic merging. If mergers

³This represents the limit case where energy losses affect the internal energies of the progenitor galaxies *before* they merge. In the other limit case the two galaxies would merge without dissipation, and then a fraction $(1 + f)\eta$ of the resulting total gas mass and of the internal energy $U_0 = -\alpha_0(E_1 + E_2)/(1 + \alpha_0)$ would be dissipated, where $\alpha_0 = (M_{g1} + M_{g2})/(M_{*1} + M_{*2})$. The two schemes lead to identical predictions when $\alpha_1 = \alpha_2$, or, for $\alpha_1 \neq \alpha_2$, when $\sigma_1 = \sigma_2$.

involve galaxies on bound orbits, the additional negative energy term in equation (15) would lead to an increase of σ_v also in equal-mass dry mergers. The analysis of this case, and the question of how much fine-tuned the properties of the progenitor galaxies should be with their binding orbital energy in order to reproduce the scaling laws, are not further discussed in this paper (e.g., see Boylan-Kolchin et al. 2005, 2006; Almeida, Baugh & Lacey 2006).

2.1. Relating intrinsic to observational properties: weak homology effects

So far the discussion involved galaxy virial properties only. However, galaxy scaling laws relate observational quantities such as total luminosity L , central projected velocity dispersion σ (luminosity averaged over some aperture), and circularized effective radius R_e . For example, in this paper we compare our models with the FJ ($L \propto \sigma^{3.92}$, rms[log σ]=0.075), Kormendy ($L \propto R_e^{1.58}$, rms[log R_e]=0.1), and edge-on FP⁴ ($R_e \propto \sigma^{1.51} I_e^{-0.77}$, rms[log R_e] = 0.049) relations in the z-band as given by Bernardi et al. (2003a,b); we also consider the $M_{BH} - \sigma$ relation (Ferrarese & Merritt 2000; Gebhardt et al. 2000). An important issue of the present analysis is then how to map, for each galaxy model, the two sets (M_*, r_v, σ_v) and (L, R_e, σ) .

Because we are not using N -body simulations – where under the assumption of a constant mass-to-light ratio Υ_* the relation between virial and ”observed” properties is known (e.g., see NLC03) – we adopt a conservative approach, and we assume a mass-dependent structural *weak homology* of our galaxies compatible with the FP tilt (e.g., see BCD02): in practice, we ”force” the models to stay on the edge-on FP, and then we check if and how the FJ and Kormendy relations are preserved. This assumption is well founded, both observationally and theoretically. In fact, it is known that the edge-on FP is characterized by a tilt, i.e., by a systematic trend of the ratio between the stellar mass-to-light ratio Υ_* and the virial parameter K_v

$$\frac{\Upsilon_*}{K_v} \propto L^{-\frac{\alpha+2\beta}{\alpha}} R_e^{\frac{2+\alpha+4\beta}{\alpha}}, \quad (20)$$

where $GM_* = K_v R_e \sigma^2$, and identity above holds for the general expression of the edge-on FP $\log R_e = \alpha \log \sigma + \beta \log I_e + \gamma$ (curiously, we note that while in the B-band all the tilt depends on luminosity (BCD02), in the present case and in the K-band it is almost due only to R_e , with $\Upsilon_*/K_v \propto L^{0.02} R_e^{0.28}$ (e.g., see Treu 2001). Unfortunately, a definite answer about the origin and the physical driving parameter(s) of the FP tilt is still missing. It is however

⁴Note that the slopes of the three considered scaling laws are mutually consistent within the errors, i.e., the combination of the FJ and the Kormendy relations gives the adopted edge-on FP best fit. Similar results are obtained using the K-band relations of Pahre et al. (1998).

known that structural weak homology could be able to produce the whole (or a large part of) the FP tilt. In particular, Sersic (1968) models provide a remarkably good description of the light-profiles of elliptical galaxies (e.g., see Caon et al. 1993, Graham & Colless 1997), with the Sersic index n increasing with galaxy luminosity and spanning the range of values required by equation (20) to reproduce the FP tilt (e.g., see Ciotti, Lanzoni & Renzini 1996, Ciotti & Lanzoni 1997, BCD02). Note that an increase of n with galaxy mass was also found in N -body simulations of major mergers (NLC03). Thus, in this paper we introduce weak homology by assuming that for a galaxy characterized by the pair (r_v, σ_v) , the observables R_e and σ are given by

$$\frac{r_v}{R_e} \simeq \frac{250.26 + 7.15n}{77.73 + n^2}, \quad (21)$$

and

$$\frac{\sigma}{\sigma_v} \simeq \frac{24.31 + 1.91n + n^2}{44.23 + 0.025n + 0.99n^2}. \quad (22)$$

The two relations above, where σ is the luminosity wheighted projected velocity dispersion within $R_e/8$, hold with very good accuracy for one-component, isotropic Sersic models with $2 \lesssim n \lesssim 12$ (Ciotti 1991, Ciotti & Lanzoni 1997, Ciotti & Bertin 1999). From equations (21) and (22) the corresponding virial coefficient $K_v(n) = (r_v/R_e) \times (\sigma_v/\sigma)^2$ is easily found (see also CBD02). How a specific value of n is assigned to a given galaxy model is described in the following Sections.

2.2. Equal mass merging

In order to illustrate the effect of repeated dry and wet mergers on a population of elliptical galaxies, in this Section we start our analysis presenting the idealized case of a merging hierarchy of equal mass spheroids, extending the analysis of CvA01 to the dissipative case. The seed galaxies (zeroth-order generation) are identical systems characterized by a stellar mass M_{*0} , a gas mass $M_{g0} = \alpha_0 M_{*0}$, a central BH mass $M_{BH0} = \mu_0 M_{*0}$, a virial radius r_0 , and a virial velocity dispersion σ_0 . A galaxy of the i -th generation is the merger-product of two galaxies of $(i - 1)$ -th generation, so the equations (10)-(19) can be written in recursive form. The solution of the gas mass equation (12), that in the present case reads $M_{gi+1} = 2(1 - \eta - f\eta)M_{gi}$, is

$$M_{gi} = (2q)^i M_{g0}, \quad q \equiv 1 - \eta - f\eta, \quad (23)$$

so that for $q \leq 1/2$ the gas mass is a steadily decreasing quantity along the merging hierarchy. The stellar mass equation (10) becomes $M_{*i+1} = 2M_{*i} + 2\eta M_{gi}$, and from equation (23) we obtain

$$M_{*i} = 2^i \left(1 + \alpha_0 \frac{1 - q^i}{1 + f} \right) M_{*0}, \quad (24)$$

while the gas-to-star mass fraction at stage i is given by

$$\alpha_i = \frac{\alpha_0 q^i (1 + f)}{1 + f + \alpha_0 (1 - q^i)}; \quad (25)$$

at variance with M_{gi} , α_i is a decreasing function of i independently of the value of q . In Fig.1 we show the evolution of α_i along sequences of ten equal-mass mergers, starting from gas-dominated seed galaxies ($\alpha_0 = 4$) and for different values of η (with $f = 10^{-3}$): according to equation (24) the stellar mass increases by a factor $\sim 10^3$ for $\eta = 0$ and of $\sim 5 \times 10^3$ for $\eta = 0.9$. The horizontal solid line $\alpha_i = \alpha_0$ represents the dry merging case ($\eta = 0$; note that we call “wet” a merging in which gas dissipation is active: a gas rich merger with $\eta = 0$ is in practice a dry merger). When significant dissipation is present, α_i dramatically decreases in the first mergers for the combined effects of gas depletion and the associated stellar mass increase. Only for values of η as low as ~ 0.1 a more gentle evolution is produced.

The BH mass evolution equation (11), $M_{BH i+1} = 2^{1/p} M_{BH i} + 2f\eta M_{gi}$, is solved with the aid of equation (23) and reads

$$M_{BH i} = 2^{i/p} M_{BH 0} \times \begin{cases} 1 + \frac{f\eta\alpha_0}{\mu_0} \frac{2^{i(1-1/p)} q^i - 1}{q - 2^{1/p-1}}, & q \neq 2^{1/p-1}; \\ 1 + \frac{f\eta\alpha_0}{\mu_0} 2^{1-1/p} i, & q = 2^{1/p-1}; \end{cases} \quad (26)$$

the explicit formula of the BH-to-star mass ratio μ_i (equation [14]) can be derived from equation (24) and the equation above. The evolution of μ_i is shown in the middle panel of Fig.1 for the maximally radiative case $p = 2$ and for fixed $f = \mu_0 = 10^{-3}$: while the Magorrian relation is preserved by construction in case of classical BH merging ($p = 1$, solid horizontal line), in the extreme ($p = 2$) case μ_i decreases for increasing galaxy mass, even though fresh gas is added to the BH at each merging in proportion to the stellar mass increase. Thus, in order to preserve the Magorrian relation when $p > 1$, an increasing fraction $f\eta$ of the available gas must be accreted on the BH as the merging hierarchy proceeds, increasing the AGN activity. When the progenitor spheroids are gas rich, high values of η may initially compensate the decrease of μ due to gravitational radiation; however, after a few mergers these galaxies run out of gas, and the final values of μ are even lower than in the less dissipative $\eta = 0.1$ case.

From equations (16) and (17) we finally obtain the relations between the virial velocity dispersion and the virial radius of the progenitors and of the new galaxy:

$$\frac{\sigma_{vi}^2}{\sigma_{vi-1}^2} = 1 + \frac{\eta(1 + 2f)\alpha_{i-1}}{1 + (1 - f\eta)\alpha_{i-1}}, \quad (27)$$

$$\frac{r_{vi}}{r_{vi-1}} = \frac{2[1 + (1 - f\eta)\alpha_{i-1}]^2}{(1 + \alpha_{i-1})[1 + \alpha_{i-1} + \eta(1 + f)\alpha_{i-1}]}. \quad (28)$$

As expected, σ_v is larger (and r_v is smaller) in the wet than in the dry merging case: for example, $\sigma_{vi}^2 \sim \sigma_{vi-1}^2 (1 + \eta)$ and $r_{vi} \sim 2 r_{vi-1} / (1 + \eta)$ in the limit of $\alpha_{i-1} \gg 1$. Figure 1 shows how gas dissipation may produce a non-monothonic behavior of the quantity $\langle f_* \rangle_i \equiv \langle \rho_* \rangle_i / \sigma_{vi}^3 = 3 M_{*i} / (8 \pi r_{vi}^3 \sigma_{vi}^3)$, which is often considered an estimate of the phase-space density. In particular, while $\langle f_* \rangle_i$ decreases as $\langle f_* \rangle_0 / 4^i$ in equal mass dry merging, in highly dissipative gas rich mergers the increase of $\langle \rho_* \rangle$ dominates over the increase of σ_v^3 , and $\langle f_* \rangle_i \sim \langle f_* \rangle_{i-1} (1 + \eta \alpha_{i-1}) (1 + \eta)^{3/2} / 4$. From the previous formula one would then conclude that an increase of the phase-space density is limited to exceptionally gas rich mergers, but this is not correct. In fact $\langle f_* \rangle$ is based on virial quantities, that by their nature refer to global scales: an increase of the phase-space density in the galactic central regions can be produced by the *localized* dissipation of a smaller amount of gas.

In Fig.2 we plot the representative points of the same models of Fig.1 in the (M_*, σ) , (M_*, R_e) , (M_*, R_e, σ) , and (M_{BH}, σ) planes. These plots, under the assumption of the same stellar mass-to-light ratio Υ_* for all models, correspond to the FJ (panel a), Kormendy (panel b), and FP (panel c) planes. The assumption of a constant value for Υ_* is made less severe by the comparing the models to the observed scaling laws in the z-band (dashed lines), where metallicity effects on Υ_* are reduced with respect to bluer wavelengths. Merging induced structural weak homology is imposed by assuming that the seed galaxies are Sersic $n = 2$ models in accordance with the observed light profiles of low-luminosity ellipticals, and that n increases by 1 in each merging, as shown by numerical simulations (NLC03). In this way, the final range of values spanned by n is between 2 and 12, consistently with observations. In practice, for assigned values of r_0 and σ_0 of the seed galaxies, from equations (21) and (22) with $n = 2$ we obtain their R_e and σ . We also assume that the seed galaxies are placed at the lower end of the various scaling laws represented in Fig. 2. The equal mass merging formula (27)-(28) are then applied, and the new virial radius and velocity dispersion are mapped in the corresponding R_e and σ again from equations (21) and (22) with $n = 3$, and so on.

From Fig.2c it is apparent how the FP tilt is well reproduced by the models corresponding to dry mergers (solid dots). The adopted prescription for weak homology is relevant here: in fact, it is easy to prove that if the models were plotted by using r_v and σ_v instead of the fiducial R_e and σ , they would be placed along a line of slope $-1/\beta \sim 1.3$ (for a surface-brightness coefficient $\beta = -0.77$ in the FP expression) instead of 1. Figure 2c also shows that highly dissipative wet mergers are initially displaced from the FP, but they again move along lines almost parallel to the edge-on FP as soon as a large fraction of gas is converted into stars. These simple considerations indicate that the final position of a galaxy in the FP space as a consequence of merging is sensitive to the physical processes involved, as already discussed by Bender, Burstein & Faber (1993). At variance with the edge-on

FP, neither the FJ nor the Kormendy relations are reproduced: in particular, while velocity dispersions are too low, effective radii are too large. Again, note that this inconsistency would be exacerbated when plotting r_v and σ_v : for example, solid dots in Fig.2a would be aligned on a horizontal line, while in Fig.2b they would be placed on the line $r_v \propto M_*$. From Fig.2d it is finally apparent how the $M_{BH} - \sigma$ relation is also failed, especially in the classical merging case. Remarkably, for $p = 2$ the mass loss due to emission of gravitational waves maintains the BH mass nearer to the observed relations than the classical merging case. In general, wet mergers are in better agreement with the FJ and Kormendy relations than dry mergers (in a way dependent on the specific value of η), due to the shrinking of r_v and the increase of σ_v . Unfortunately, in the present framework we cannot evaluate the galaxy non-homology induced by gas dissipation, that can be investigated only with N-body+gas numerical simulations such those of Robertson et al. (2006a), and so weak homology is just imposed with the same prescription as for dry mergers. In any case, the preliminary analysis of this Section is consistent with the idea that the FJ and Kormendy relations are stronger tests for merging than the edge-on FP, as already clearly shown by numerical simulations (e.g., see NLC03; Boylan-Kolchin et al. 2005, 2006).

3. The simulations

In this Section we extend the previous investigation to the study of the effects of repeated parabolic merging on a *population* of elliptical galaxies. The merging spheroids are extracted by means of Monte-Carlo simulations from different samples of seed galaxies, and the properties of the resulting galaxies are determined by using the relations derived in Section 2. The motivation for these simulations is the fact that equal-mass merging maximizes (minimizes) the effects on the radius (velocity dispersion) of the resulting objects, while mergers of galaxies spanning a substantial range of masses, sizes and velocity dispersions not only are more realistic, but also could lead to less dramatic effects on the scaling relations.

In particular, we focus on two schemes designed to explore and quantify the impact of dry and wet merging on the formation and evolution of elliptical galaxies. In the first scheme the seed galaxies span only a narrow mass range (a factor of ~ 5): in this case we then study whether massive ellipticals and the observed scaling relations can be *produced* by repeated mergers of low-mass spheroidal systems. In the second scheme the seed ellipticals follow the observed scaling relations over their whole observed mass range ($\sim 10^3$), and so we explore whether repeated merging events preserve or destroy these relations. For sake of completeness, and also to check the robustness of the results obtained with the Monte-Carlo simulations, we finally conduct a third set of experiments in which the merging histories are

described by Press & Schechter (1974) merger trees.

How the mass, virial radius and velocity dispersion of the seed galaxies, as well as their effective radius and central velocity dispersion, are assigned in each experiment is described in the corresponding Sections. In all cases, however, the initial mass of the SMBH obeys the Magorrian relation with $\mu_0 = 10^{-3}$.

3.1. Merging small seed galaxies

In this first scheme, once two spheroids are extracted from the initial population (made of 1000 objects), they are merged together, and the properties of the merger end-product are computed as described in Section 2. The two progenitors are then removed from the seed galaxy population, while the new object is added to it; the procedure is repeated until the largest produced galaxies are $\sim 10^3$ times more massive than the smallest seed galaxy in the original sample. This may require up to 10-12 mergers, ~ 7 -10 of which being major mergers (i.e., merging in which the stellar mass ratio of the progenitors is in the range 0.3–3; e.g., see Kauffmann, Guiderdoni & White 1994). The initial population of seed galaxies is obtained by random extraction (with the von Neumann rejection technique) of the stellar mass M_* from the SDSS z-band galaxy luminosity function (Blanton et al. 2001), under the assumption of constant stellar mass-to-light ratio Υ_* . Finally, the mass ratio of the most massive to the less massive galaxy in the sample is taken to be 5. In case of wet mergers, the *total* (stars+gas) mass is the quantity which is extracted. For each galaxy mass, the corresponding central velocity dispersion σ is fixed according to the z-band FJ, and the effective radius R_e is assigned from the FP in the z-band (Bernardi et al. 2003a,b). Due to the restricted mass range, all the galaxies are assumed to be $n = 2$ Sersic models, and so their virial radius r_v and virial velocity dispersion σ_v can be easily calculated. We then apply the rule that in major mergers the Sersic index of the resulting galaxy is $n = 1 + \max(n_1, n_2)$, where n_1 and n_2 are the Sersic indices of the progenitors. In minor mergers, the Sersic index instead keeps the same value of the more massive galaxy. Note that this is a quite conservative assumption, because in NLC03 it was found that in head-on minor mergers n actually *decreases*, producing galaxies that fall outside the edge-on FP.

Figures 3 and 4 show the results in the cases of dry ($\alpha_0 = 0$) and dissipative gas rich ($\alpha_0 = 4, \eta = 0.3$) parabolic merging, respectively; the mass interval spanned by the progenitors is indicated by the two vertical ticks, the end-product positions are represented by the dots, and the observed scaling laws are represented by the dotted lines. Figure 3 reveals that massive ellipticals cannot be formed by parabolic dry mergers of low-mass spheroids only, because they would be characterized by exceedingly large R_e and almost

mass independent σ , in agreement with the results of CvA01 and NLC03, and with the conclusions of Section 2. In fact, when galaxies reach a mass ~ 10 times larger than that of the largest seed galaxies, all the seed galaxy population can be considered made by equal mass objects, and the considerations of Section 2.2 apply.

Figure 4 shows the results in the case of wet merging of gas dominated ($\alpha_0 = 4$) galaxies. As expected, mergers with gas dissipation produce more realistic objects than dry mergings and, remarkably, the observed scaling laws are satisfied (even though with a large scatter) by the new galaxies, up to a mass increase of a factor of 10^2 with respect to the smallest seed galaxies. However, new galaxies characterized by a mass increase factor $\gtrsim 10^2$ are mainly formed by mergers of gas poor galaxies that already experienced several mergers, and so they deviate from the observed scaling laws as the galaxies in Fig.3.

More quantitatively, the models plotted in Fig.3 deviate from the observed $M_{BH} - \sigma$ and FJ relations by more than $1 - \sigma$ when their (logarithmic) mass increase is $\gtrsim 1.4$ and $\gtrsim 2.4$, respectively, the larger mass value allowed by the FJ being due to its larger scatter. The mean gas-to-star mass ratio for the deviating models is $\alpha \lesssim 0.5$ (even though several models with a lower α are still consistent with the two relations considered). Quite obviously, these values depend on the initial amount of gas: for example, when starting with $\alpha_0 = 10$ the models are incompatible with the observed $M_{BH} - \sigma$ for a logarithmic increase of the stellar mass of $\gtrsim 2.2$, and for $\alpha \lesssim 0.3$. We note, however, that the populated region in the edge-on FP is reduced for increasing α_0 , as can be seen by comparing the model distributions in Figs. 3 and 4.

This first exploration therefore reveals that parabolic merging of low mass galaxies only is unable to produce elliptical galaxies obeying the observed scaling laws, even when allowing for structural weak homology in a way consistent with the edge-on FP. However gas dissipation plays an important role in gas rich merging and remarkably the resulting elliptical galaxies appear to be distributed as the observed scaling relations, as far as enough gas is available. Quite obviously, the problem of the compatibility of the properties of such merger-products with other key observations, such as the color-magnitude and the metallicity-velocity dispersion relations, and the increasing age of the spheroids with their mass (e.g., see Renzini 2006; Gallazzi et al. 2006) cannot be addressed in the framework of this paper.

3.2. Merging "regular" galaxies

In the second scheme, the masses of the seed galaxies span the full range covered by ordinary ellipticals ($\sim 10^3$), and their characteristic size and velocity dispersion follow the observed scaling relations. The mass, effective radius, and central velocity dispersion of each seed galaxy are assigned as described in Section 3.1; however, due to the large mass range spanned in the present case, the models cannot be characterized by the same value of the Sersic index, if they are placed on the edge-on FP. For this reason a Sersic index is assigned to each seed galaxy by solving for n the equation $K_v(n) = GM_*/R_e\sigma^2$; in turn, from the knowledge of n we obtain the values of r_v and σ_v needed in the merging scheme. For simplicity we restrict our study to major mergers only, increasing by 1 the larger Sersic index characterizing each merging pair. Finally, for consistency with the imposed scaling laws (which hold for present-day gas poor spheroids), we focus on dry merging only. In this Section we then study the effect of merging on already established scaling laws.

In practice, once a galaxy is chosen, a second galaxy with a mass ratio to the first in the range $0.3 - 3$ is extracted from the seed population, and then the two galaxies are merged. As in the other cases, the intrinsic galaxy properties are transformed into their "observational" counterparts by using equations (21) and (22). The procedure is repeated by selecting a third galaxy from the initial population, and so on for a total of 6 major mergers. The positions in the observational planes of 1000 galaxies (at all stages of the merging hierarchy) are shown in Fig.5. The main result is that now, at variance with the narrow mass range experiments, the scaling laws remain almost unaffected by the merging, both in their slope and scatter. In particular, note how the $M_{BH}-\sigma$ relation (with $p = 2$) is preserved, even though we are in dry merging regime. The only detectable deviations from the observed scaling laws, for the same reasons already discussed in Section 3.1, are found for ellipticals with masses larger than the most massive galaxies in the original sample (marked by the two vertical ticks in Fig.5).

Why mergers do preserve so well the scaling relations? The reason is simple: by construction in a population of galaxies spanning the whole mass range observed today and distributed according to the observed scaling laws, mergers in general involve a "regular" elliptical, with realistic values of R_e and σ . These mergings act as a "thermostat", maintaining values of R_e in the observed range and increasing the virial velocity dispersion, thus contributing to preserve the scaling laws. Only when the produced galaxies are so massive that no regular galaxies of comparable mass are available, the new merger products deviate more and more from the scaling laws. This behavior becomes extreme in the case of repeated mergers in a galaxy population spanning a restricted mass range, as discussed in Section 3.1. Thus, our analysis confirm that while the elliptical galaxy scaling laws (and so elliptical

galaxies) cannot be produced by the merging of low mass spheroids only (as already pointed out by e.g., CvA01, NLC03, Evstigneeva et al. 2004), these relations once established by some other mechanism, are robust against merging.

3.3. Cosmological merger trees

We conclude our study by presenting a set of numerical experiments aimed at investigating the evolution of galaxies with a merging history obtained from the extended Press & Schechter (1974) formalism in a standard Λ CDM cosmology. The details of the realization of the merger trees are given in Volonteri, Haardt & Madau (2003), while the ensemble from which they have been extracted is in accordance with the Jenkins (2001) modified P&S formula. In particular, we selected a set of 20 merger trees tracing the merger history, from $z = 5$ to $z = 0$, of a halo with mass $\simeq 10^{13} M_{\odot}$ at present time. Since the mass resolution in the merger tree scales as $M_{\text{res}} = 10^{10} (1+z)^{-3.5} M_{\odot}$, it follows that M_{res} is always $\lesssim 5\%$ of the main halo mass in the merger hierarchy. This wide range of masses allows for both minor and major mergers in the tree at all redshifts. that the *statistical* discrepancies between the DM function derived from the Press & Schechter formalism and numerical simulations (e.g., Jenkins et al. 2001) are not the present context, where we focus on the growth of a

In practice, we applied at each merging event in a given tree the relations derived in Section 2, both for the dry and the wet ($\alpha_0 = 4, \eta = 0.3$) cases, for a total of 40 simulations. The virial radius r_v of each seed halo (that we arbitrarily identify with a galaxy) is now defined as the radius of the sphere characterized by mean mass density $\Delta_{\text{vir}} \rho_{\text{crit}}$ (where ρ_{crit} is the critical density for closure at redshift z , and Δ_{vir} is the density contrast at virialization⁵). This definition of virial radius is not - strictly speaking - identical to the standard dynamical relation (9). However, in Lanzoni et al. (2004) it was shown that the two definitions of r_v are in nice agreement, and so we also define the halo (galaxy) virial velocity dispersion from the virial theorem $GM = r_v \sigma_v^2$. The properties of the merger end-product are determined according to the dry or wet relations, while those of the secondary galaxy involved in each subsequent event follow the cosmological virial relations. The weak homology trend is added to the models by assigning a Sersic index $n = 2$ to the main halo at $z = 5$ (which is assumed to be placed on the reference scaling laws), and increasing it by 1 in each major merger; in minor mergers n is maintained constant.

For simplicity, in Fig.6 we show the FJ, Kormendy and FP planes for just two out of the 40 simulations, being the behavior of galaxy models in all the merger trees almost iden-

⁵For the assumed cosmology this can be approximated by $\Delta_{\text{vir}} \simeq 178 \Omega^{0.45}$ (Eke, Navarro, & Frenk 1998).

tical. Note that at variance with Figs.3,4, and 5, here the points constitute an evolutionary sequence, representing the successive positions of the main halo during its mass accretion history. From the comparison with Figs.3 and 4 it is apparent that deviations from the slope of the FJ and Kormendy relations are less strong than in the previous cases, while the evolutionary tracks of the growing halos move parallel to the edge-on FP plane.

The fact that also in the merger tree exploration the slopes of the FJ, Kormendy, and FP relations are preserved is not surprising, as it is easily explained when combining the results of previous Sections with the fact that now the "galaxies" involved in the mergings are provided by the cosmological setting, in which $M \propto r_v^3 \propto \sigma_v^3$. Thus, the determinant factor of success is again the availability of galaxies with a virial radius and velocity dispersion increasing with the halo mass, a property that cannot be produced by parabolic mergings of small systems only, but it is the natural consequence of the substantially different phenomenon of negative energy collapses (see Introduction).

Note that the accordance with observations would be in fact even better than the results shown in Fig. 6. According to the hierarchical merging picture, the number of mergers an elliptical galaxy experiences in its lifetime (efficient mergers, i.e., those with time scales shorter than the Hubble time) is much smaller than the number of halo mergers in a cosmological merger tree, as only a small fraction ($\lesssim 30\%$) of them leads to galaxy mergers, once the finite time needed for merging is taken into account (see Fig.7). In fact, dynamical friction appears to be very efficient (i.e., with a decay timescale shorter than the Hubble time) only for mergers with a mass ratio of the progenitors $\gtrsim 0.1$ (Taffoni et al. 2003), while satellites in intermediate mass ratio ($0.01 - 0.1$) suffer severe mass losses by the tidal perturbations induced by the gravitational field of the primary halo, and this progressive mass loss further increases the decay time. The lightest satellites are almost unaffected by orbital decay, so they survive and keep orbiting on rather circular, peripheral orbits.

4. Discussion and conclusions

With the aid of a scheme based on very simple physical arguments we investigated the influence of dry and wet merging on the formation and evolution of elliptical galaxies, focusing on the origin and robustness of some of their scaling laws. In particular, by using analytical arguments and numerical simulations we showed that massive elliptical galaxies cannot be formed by (parabolic) merging of low mass spheroidal galaxies, even in presence of substantial gas dissipation, and allowing for the helpful effects of structural weak homology. However the observed scaling laws of elliptical galaxies, once established by galaxy formation, are robust against merging. More specifically, our findings can be summarized as follows:

1) Parabolic dry merging in a population of low mass spheroids leads to massive ellipticals that cannot be simultaneously placed on the Kormendy, FJ and edge-on FP relations. For example, forcing the end-products to stay on the edge-on FP, the FJ and Kormendy relations are failed by massive galaxies, with deviations increasing with galaxy mass. This behavior was predicted in CvA01 and confirmed by high resolution numerical simulations (NLC03, Boylan-Kolchin et al. 2005, 2006). For example Boylan-Kolchin et al. (2006), in a series of dissipationless merging simulations of galaxies in cosmologically motivated orbits, found that the merging end-products, while preserving the edge-on view of the FP, can present significant differences in the FJ and Kormendy relations. This because the variations in the resulting $M_* - R_e$ are compensated by corresponding variations in the $M_* - \sigma$ relation, so that the *projections* of the FP - but not the edge-on FP itself - should provide a powerful way to investigate the assembly history of massive elliptical galaxies.

2) Parabolic wet merging in the same population of low mass progenitors lead to galaxies in much better agreement with the observed scaling relations, as long as enough gas for dissipation is available. In particular, the resulting $M_{BH} - \sigma$ relation is in better agreement with the observed one, also in the case of significant mass loss (via gravitational waves) of the coalescing BHs. Significant deviations from the observed scaling laws are however expected for massive galaxies. Similar conclusions were reached by sophisticated N -body plus hydrodynamical simulations of merging of disk galaxies. For example, Kazantzidis et al. (2005) found that merging disk galaxies constructed to obey the $M_{BH} - \sigma$ relation move relative to it depending on whether they undergo a dissipational or dissipationless merger. In particular, remnants of dry mergings tend to move away from the mean relation, showing the role of gas-poor mergers as a possible source of scatter. In addition, Robertson et al (2006b) studied the development of the $M_{BH} - \sigma$ over cosmic time with a large set of hydrodynamical simulations of galaxy mergers that include star formation and feedback from the growth of the central BH, and found that the $M_{BH} - \sigma$ relation is created through coupled BH and spheroid growth (via star formation) in galaxy mergers.

3) Parabolic dry mergers in a population of galaxies following the observed scaling laws over the full mass range populated today by stellar spheroids (or following the scaling laws of dark matter halos predicted by the current cosmological scenario), preserve the Kormendy, FJ, and edge-on FP remarkably well. The reason of this behavior is rooted in the availability in the merger population of galaxies with velocity dispersion increasing with galaxy mass. Remarkably, Robertson et al. (2006a) found evidences that dry merging of spheroidal galaxies at low redshift is expected to maintain the FP relation *imprinted by gas-rich merging during the epoch of rapid spheroid and central BH growth at high redshift*, when the progenitors were characterized by gas fractions $\gtrsim 30\%$ and efficient gas cooling was allowed in the simulations.

Thus, points 1) and 2) above suggest that ellipticals cannot be originated by parabolic merging of low mass spheroids only, even in presence of substantial gas dissipation. In addition, point 3), when considered together the cosmologically imprinted scaling laws of dark matter halos, and the several appealing features of dissipationless collapse end-products (see Introduction), support the idea that elliptical galaxies formed in a process similar to the monolithic collapse, even though their structural and dynamical properties are compatible with a limited number of dry mergers (we note that the same conclusion has been reached also from the study of color profiles in early-type galaxies, as described in Wu et al. 2005).

The possibility that monolithic collapse and successive merging are just the leading physical processes at different times in galaxy evolution, and that they are both important for galaxy formation, is perhaps indicated also by a "contradictory" and often overlooked peculiarity of massive ellipticals. In fact, while the Kormendy relation dictates that the mean stellar density of galaxies decreases for increasing galaxy mass (a natural result of parabolic dry merging), the normalized light profiles of elliptical galaxies becomes steeper and their metallicity increases at increasing galaxy mass (as expected in case of significant gas dissipation). Thus, the present-day light profiles of ellipticals could represent the fossil evidence of the impact of both the processes; quite obviously, this problem cannot be addressed in the framework adopted in this paper. It would be very interesting to extend the Robertson et al. (2006a) and Naab et al. (2006) analysis to the study of dissipative collapses in cosmologically motivated dark matter halos, thus extending the investigation of Nipoti et al. (2006) towards the very early phases of galaxy formation.

We thank the anonymous Referee for useful comments that improved the presentation of the paper. L.C. acknowledges the warm hospitality of the Theoretical Astrophysics Division of Harvard-Smithsonian Center for Astrophysics, where a large part of this work was carried out. Lars Hernquist, Jerry Ostriker, Brant Robertson and Tjeerd van Albada provided insightful comments. L.C. is supported by MIUR, grant CoFin2004.

REFERENCES

- Aguilar, L.A., & Merritt, D. 1990, *ApJ*, 354, 33
- Almeida, C., Baugh, C.M., & Lacey, C.G. 2006, preprint (astro-ph/0608544)
- Bell, E.F., et al. 2004, *ApJ*, 608, 752
- Bell, E.F., et al. 2006, *ApJ*, 640, 241

- Bender, R., Burstein, D., & Faber, S.M. 1993, *ApJ*, 411, 153
- Benson, A.J. 2005, *MNRAS*, 358, 551
- Bernardi, M., et al. 2003a, *AJ*, 125, 1849
- Bernardi, M., et al. 2003b, *AJ*, 125, 1866
- Bernardi, M., et al. 2003c, *AJ*, 125, 1882
- Bertin, G., Ciotti, L., & Del Principe, M. 2002, *A&A*, 386, 149 (BCD02)
- Blanton, M.R., Dalcanton, J., Eisenstein, D., et al. 2001, *AJ*, 121, 2358
- Bower, R.G., Lucey, J.R., & Ellis, R.S. 1992, *MNRAS*, 254, 589
- Boylan-Kolchin, M., Ma, C.-P., & Quataert, E. 2005, *MNRAS*, 362, 184
- Boylan-Kolchin, M., Ma, C.-P., & Quataert, E. 2006, *MNRAS*, 369, 1081
- Burkert, A., & Silk, J. 2001, *ApJ*, 554, L151
- Burstein, D., Bender, R., Faber, S., & Nolthenius, R. 1997, *AJ*, 114, 1365
- Caon, N., Capaccioli, M., & D’Onofrio, M. 1993, *MNRAS*, 265, 1013
- Capelato, H.V., de Carvalho, R.R., & Carlberg, R.G. 1995, *ApJ*, 451, 525
- Cavaliere, A., & Vittorini, V. 2002, *ApJ*, 570, 114
- Ciotti, L. 1991, *A&A*, 249, 99
- Ciotti, L., & Bertin, G. 1999, *A&A*, 352, 447
- Ciotti, L., & Lanzoni, B. 1997, *A&A*, 321, 724
- Ciotti, L., Lanzoni, B., & Renzini, A. 1996, *MNRAS*, 281, 1
- Ciotti, L., & van Albada, T.S. 2001, *ApJ*, 552, L13 (CvA01)
- Conselice, C.J., 2006, *ApJ*, 638, 686
- Dantas, C.C., Capelato, H.V., Ribeiro, A.L.B., & de Carvalho, R.R. 2003, *MNRAS*, 340, 398
- Dekel, A., & Cox, T.J. 2006, preprint (astro-ph/0603497)
- de Vaucouleurs, G. 1948, *Ann. d’Astroph.*, 11, 247

- de Zeeuw, P.T. 2001, In Black holes in binaries and galactic nuclei: diagnostics, demography and formation, ESO Astrophysics Symposia, L. Kaper, E.P.J. van den Heuvel, and P.A. Woudt editors. Springer-Verlag, p.78
- Djorgovski, S., & Davis, M. 1987, *ApJ*, 313, 59
- Dressler, A., Lynden-Bell, D., Burstein, D., Davies, R.L., Faber, S.M., Terlevich, R., & Wegner, G. 1987, *ApJ*, 313, 42
- Eggen, O.J., Lynden-Bell, D., & Sandage, A.R. 1962, *ApJ*, 136, 748
- Eke, V.R., Navarro, J.F., & Frenk, C.S. 1998, *ApJ*, 503, 569
- Evstigneeva, E.A., Reshetnikov, V.P., & Sotnikova, N.Ya. 2002, *A&A*, 381, 6
- Evstigneeva, E.A., de Carvalhho, R.R., Ribeiro, A.L., Capelato, H.V. 2004, *MNRAS*, 349, 1052
- Faber, S.M., & Jackson, R.E. 1976, *ApJ*, 204, 668 (FJ)
- Faber, S.M., et al. 2005, preprint (astro-ph/0506044)
- Ferrarese, L., & Merritt D. 2000, *ApJ*, 539, L9
- Ferrarese, L., van den Bosch, F.C., Ford, H.C., Jaffe, W., O’Connell, R.W. 1994, *AJ*, 108, 1598
- Gallazzi, A., Charlot, S., Brinchmann, J., & White, S.D.M. 2006, *MNRAS*, 370, 1106
- Gebhardt, K., et al. 2000, *ApJ*, 539, L13
- González-García, A.C., & van Albada, T.S. 2003, *MNRAS*, 342, L36
- Graham, A., & Colless, M. 1997, *MNRAS*, 287, 221
- Graham, A.W., & Guzmán, R. 2003, *AJ*, 125, 2936
- Graham, A.W., Erwin, P., Trujillo, I., & Asensio Ramos, A. 2003, *AJ*, 125, 2951
- Guzman, R., Lucey, J.R., Carter, D., & Terlevich, R.J. 1992, *MNRAS*, 257, 187
- Haehnelt, M.G., & Kauffmann, G. 2000, *MNRAS*, 318, L35
- Haiman, Z., Ciotti, L., & Ostriker, J.P., 2004, *ApJ*, 606, 763
- Hozumi, S., Burkert, A., & Fujiwara, T. 2000, *MNRAS*, 311, 377

- Hughes, S.A., & Blandford, R.D. 2003, *ApJ*, 585, L101
- Jenkins, A. Frenk, C.S., White, S.D.M., Colberg, J.M., Cole, S., Evrard, A.E., Couchman, H.M.P., & Yoshida, N. 2001, *MNRAS*, 321, 372
- Jørgensen, I. 1999, *MNRAS*, 306, 607
- Kauffmann, G., Guiderdoni, B., & White, S.D.M. 1994, *MNRAS*, 267, 981
- Kazantzidis, S., Mayer, L., Colpi, M., Madau, P., Debattista, V.P., Wadsley, J., Stadel, J., Quinn, T., & Moore, B. 2005, *ApJ*, 623, L67
- Khochfar, S., & Burkert, A. 2006, *A&A*, 445, 403
- Kormendy, J. 1977, *ApJ*, 218, 333
- Lanzoni, B., Ciotti, L., Cappi, A., Tormen, G., & Zamorani, G. 2004, *ApJ*, 600, 640
- Lauer, T.R., et al. 1995, *AJ*, 110, 2622
- Londrillo, P., Messina, A., & Stiavelli, M. 1991, *MNRAS*, 250, 54
- Mc Glynn, T.A. 1984, *ApJ*, 281, 13
- Magorrian J., et al. 1998, *AJ*, 115, 2285
- Matteucci, F. 1994, *A&A*, 288, 55
- May, A., & van Albada, T.S. 1984, *MNRAS*, 209, 15
- Naab, T., Johansson, P.H., Ostriker, J.P., & Efstathiou, G. 2006, preprint (astro-ph/0512235)
- Nipoti, C., Londrillo, P., & Ciotti, L. 2003, *MNRAS*, 342, 501 (NLC03)
- Nipoti, C., Londrillo, P., & Ciotti, L. 2006, *MNRAS*, 370, 681
- Oñorbe, J., Domínguez-Tenreiro, R., Sáiz, A., Serna, A., & Artal, H. 2005, *ApJ*, 632, L57
- Oñorbe, J., Domínguez-Tenreiro, R., Sáiz, A., Artal, H., & Serna, A. 2006, preprint (astro-ph/0609499)
- Ostriker, J.P. 1980, *Comments on Astrophys.*, 8, 177
- Pahre, M.A., Djorgovski, S.G., & de Carvalho, R.R. 1998, *AJ*, 116, 159

- Peebles, P.J.E. 1980, *The Large-Scale Structure of the Universe* (Princeton: Princeton Univ. Press)
- Pentericci, L., Ciotti, L., & Renzini, A. 1996, *Astrophysical Letters and Communications*, 33, 213
- Pipino, A., Matteucci, F. 2004, *MNRAS*, 347, 968
- Press, W.H., & Schechter, P. 1974, *ApJ*, 187, 425
- Prugniel, P., & Simien, F. 1997, *A&A*, 321, 111
- Renzini, A. 2006, *ARA&A*, 44, 141
- Robertson, B., Cox, T.J., Hernquist, L., Franx, M., Hopkins, P.F., Martini, P., & Springel, V. 2006a, *ApJ*, 641, 21
- Robertson, B., Hernquist, L., Cox, T.J., Di Matteo, T., Hopkins, P.F., Martini, P., & Springel, V. 2006b, *ApJ*, 641, 90
- Saglia, R., Maraston, C., Greggio, L., Bender, R., & Ziegler, B., 2000, *A&A*, 360, 911
- Sáiz, A., Domínguez-Tenreiro, R., & Serna, A. 2004, *ApJ*, 601, L131
- Sérsic, J.L. 1968, *Atlas de galaxias australes*. Observatorio Astronomico, Cordoba
- Shen, S., Mo, H.J., White, S.D.M., et al. 2003, *MNRAS*, 343, 978
- Taffoni, G., Mayer, L., Colpi, M., & Governato, F. 2003, *MNRAS*, 341, 434
- Thomas, D., Greggio, L., & Bender, R. 1999, *MNRAS*, 302, 537
- Toomre, A. 1977, in *Evolution of Galaxies and Stellar Populations*, Ed. B.M. Tinsley & R.B. Larson (New Haven: Yale University Observatory), p.401
- Trenti, M., Bertin, G., & van Albada, T.S. 2005, *A&A*, 433, 57
- Treu, T. 2001, PhD Thesis, Scuola Normale Superiore di Pisa, Italy
- Trujillo, I., Erwin, P., Asensio Ramos, A., & Graham, A.W. 2004, *AJ*, 127, 1917
- Udry, S. 1993, *A&A*, 268, 35
- van Albada, T.S. 1982, *MNRAS*, 201, 939
- van Dokkum, P.G. 2005, *AJ*, 130, 264

Volonteri, M., Haardt, F., & Madau, P. 2003, *ApJ*, 582, 559

White, S.D.M., & Frenk, C.S. 1991, *ApJ*, 379, 52

Wu, H., Shao, Z., Mo, H.J., Xia, X., & Deng, Z. 2005, *ApJ*, 622, 244

Yu, Q., & Tremaine, S. 2002, *MNRAS*, 335, 965

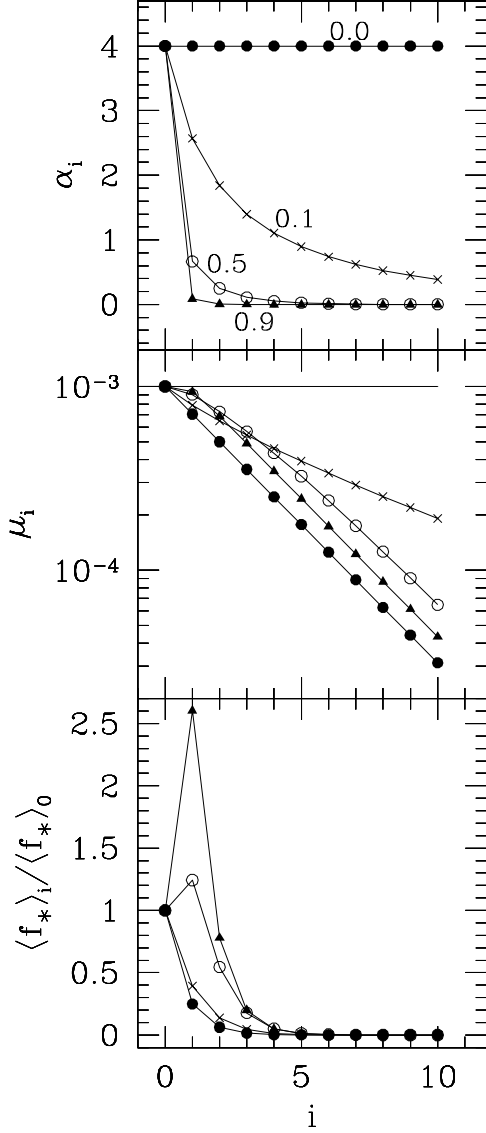


Fig. 1.— The evolution of the gas-to-star mass ratio α_i (top panel), of the BH-to-star mass ratio μ_i (middle panel), and of the stellar mean phase-space density $\langle f_* \rangle_i \equiv \langle \rho_* \rangle_i / \sigma_{vi}^3$ (bottom panel) in the case of 10 successive equal-mass parabolic mergers, and for different values of the dissipation parameter η (0, solid dots; 0.1, crosses; 0.5 empty circles; 0.9, solid triangles). In all the merging sequences, $\alpha_0 \equiv M_{g0}/M_{*0} = 4$, and $f = \mu_0 = 10^{-3}$. Maximum radiative efficiency ($p = 2$) is assumed for the BH coalescence law in the middle panel ($p = 1$ case is represented by the horizontal line).

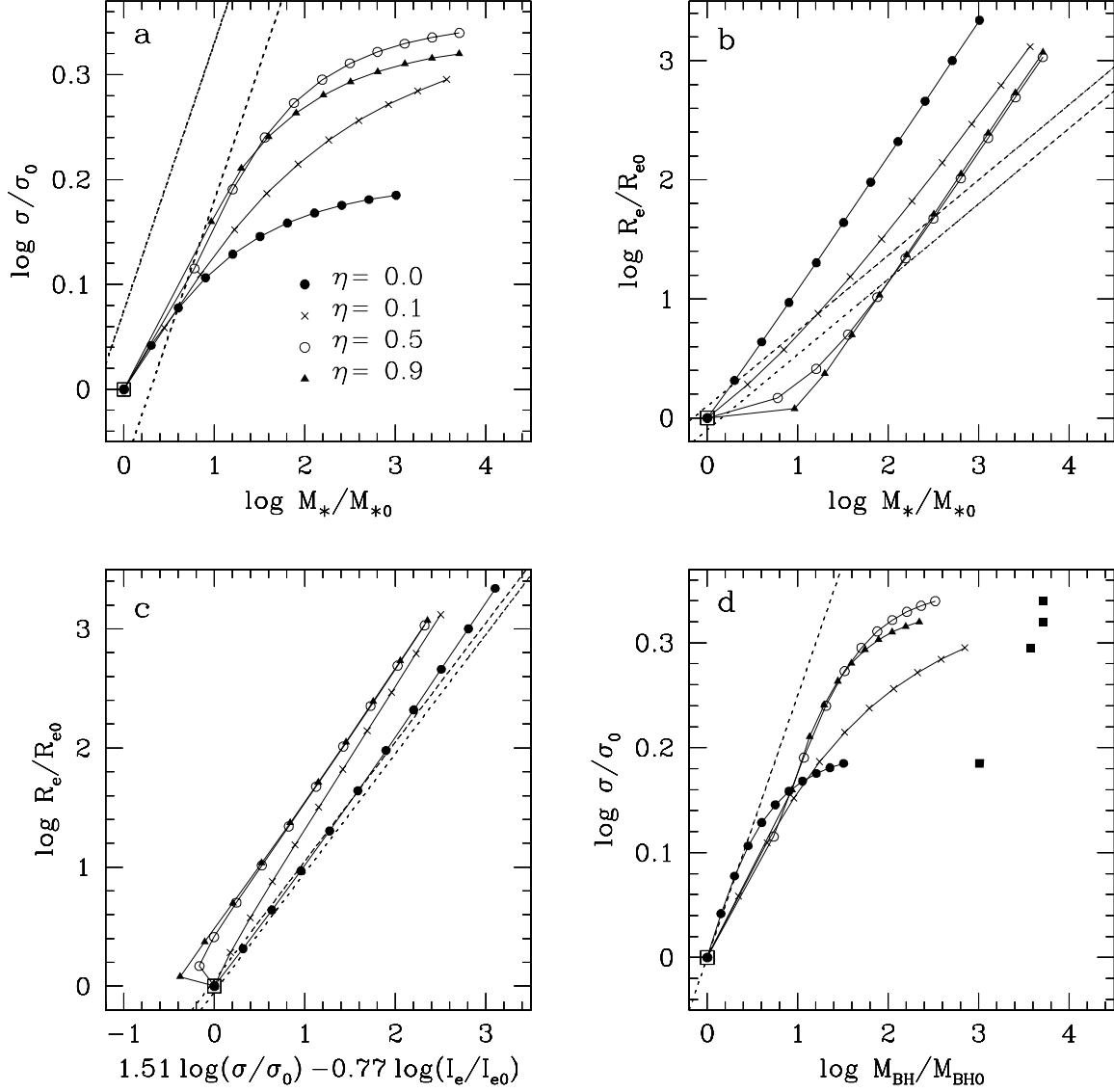


Fig. 2.— The models of Fig.1 in the scaling relation planes. Dotted lines in panels *a–c* represent the observed scaling relations in the *z*-band with their 1-rms scatter. In panel *d* the $M_{BH} - \sigma$ relation is plotted without scatter, and $p = 2$ is assumed for the BH coalescence formula, while black squares mark the position of the last merger product if $p = 1$. See Section 2.2 for details.

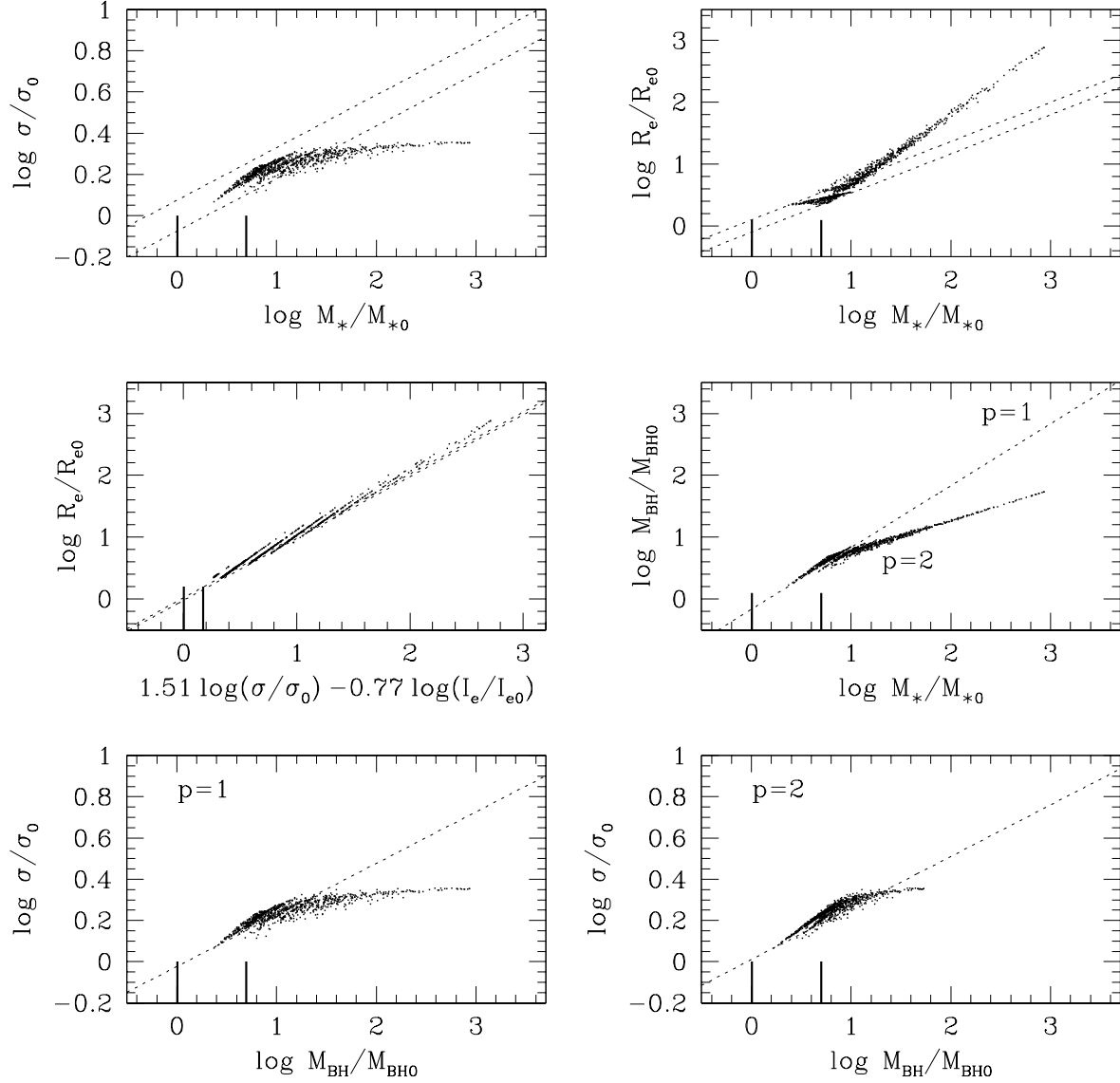


Fig. 3.— Synthetic scaling relations produced by parabolic dry mergers. Seed galaxies span a limited mass range (indicated by the heavy vertical ticks) and random re-merging events are repeated until a factor 10^3 increase in mass is reached (see text for details). Dotted lines represent the observed scaling relations, as in Fig.2. All quantities are normalized to the properties of the lowest mass seed galaxy.

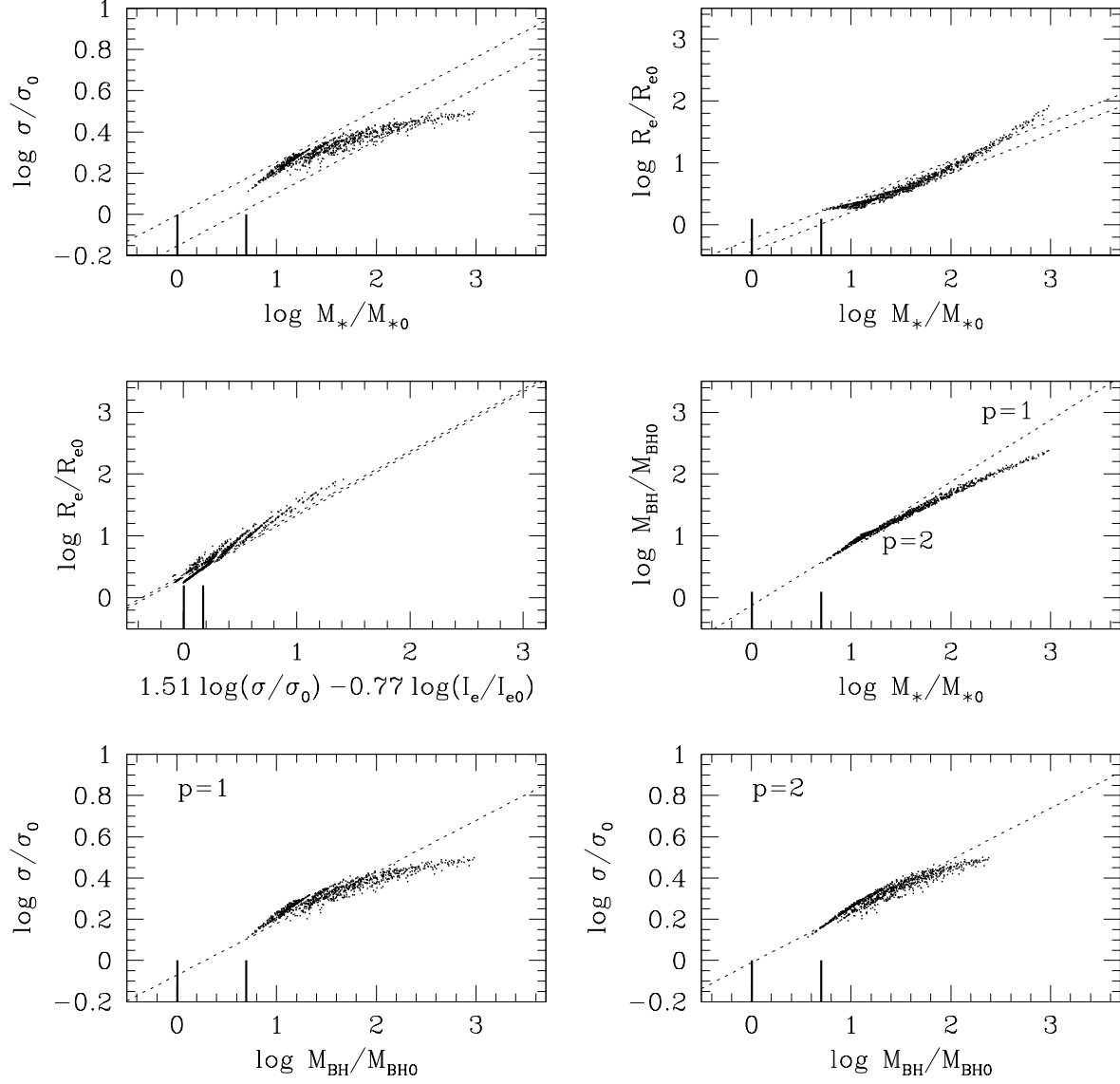


Fig. 4.— As in Fig.3, but for the wet merging of initially gas-rich galaxies: $\alpha_0 = 4$ and $\eta = 0.3$.

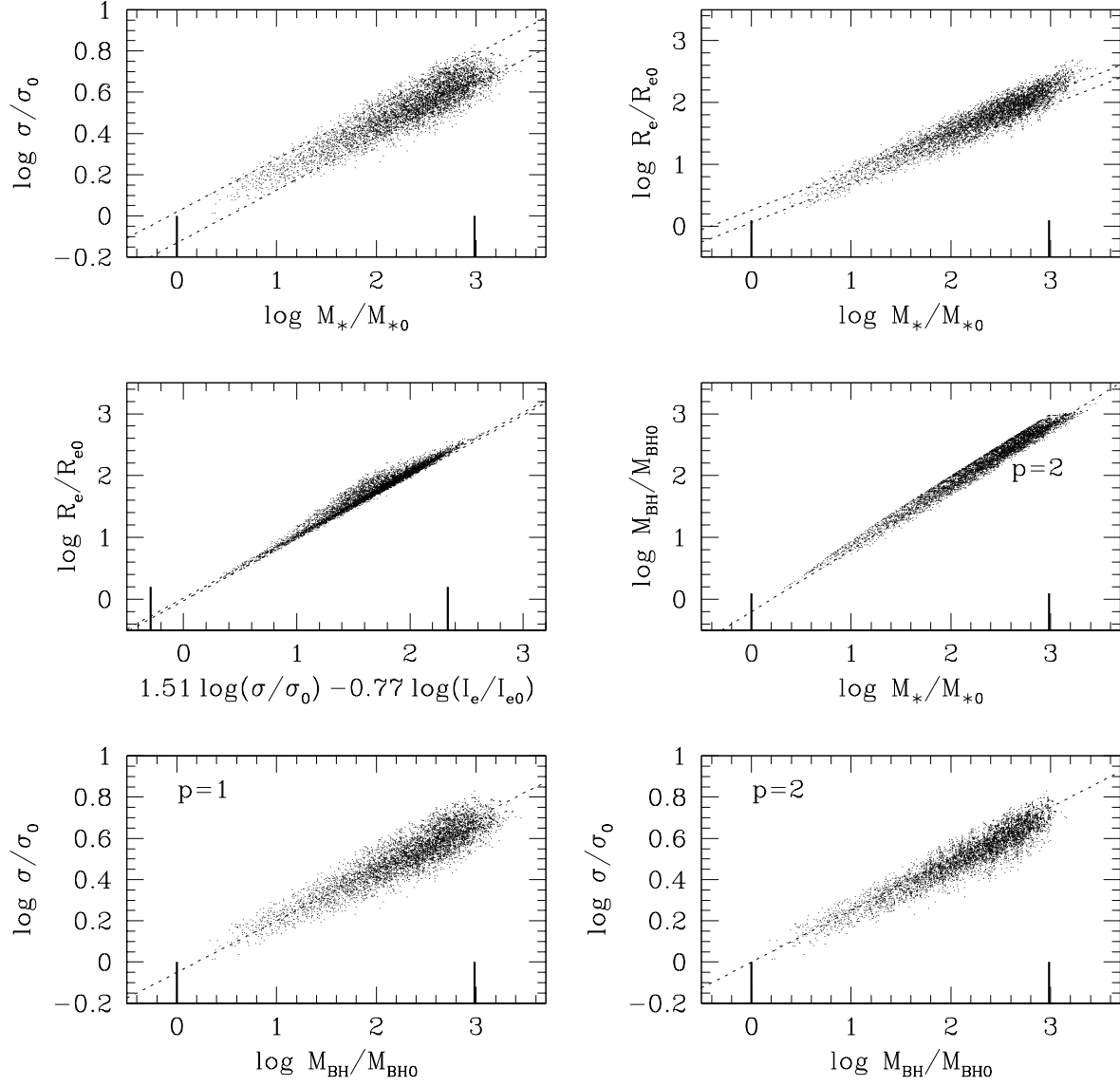


Fig. 5.— Synthetic scaling relations for the merger-products of up to 6 dry major mergers of galaxies extracted from a population that follows the observed scaling laws. Lines are as in Fig.2 and all quantities are normalized to the properties of the lowest-mass seed galaxy.

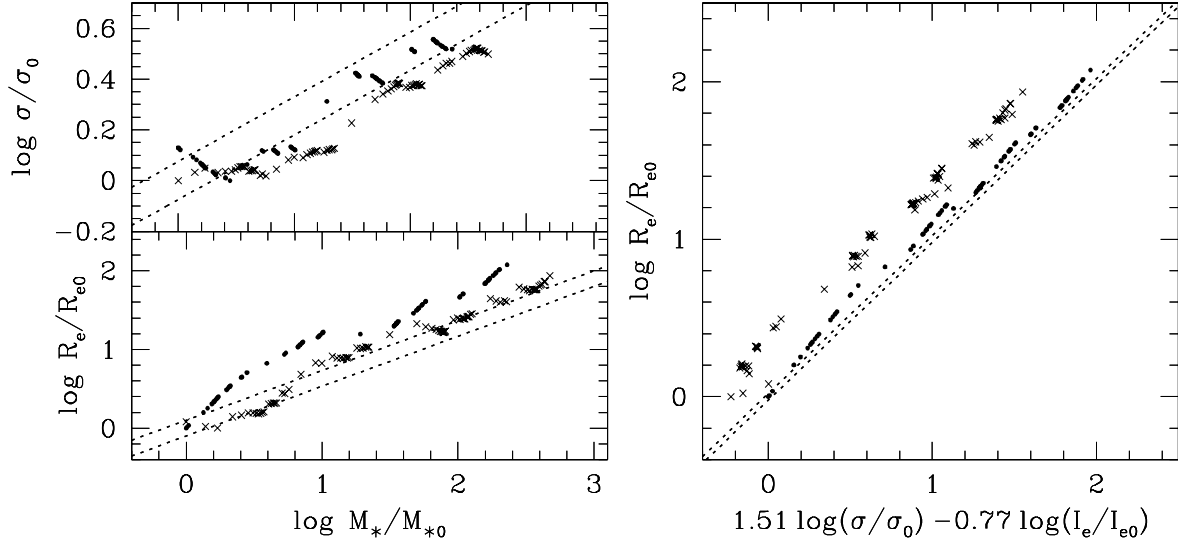


Fig. 6.— Evolutionary sequences of a main halo in the scaling law planes, according to a Press & Schechter merger tree, in the dry (dots) and wet ($\alpha_0 = 4$ and $\eta = 0.3$; crosses) cases.

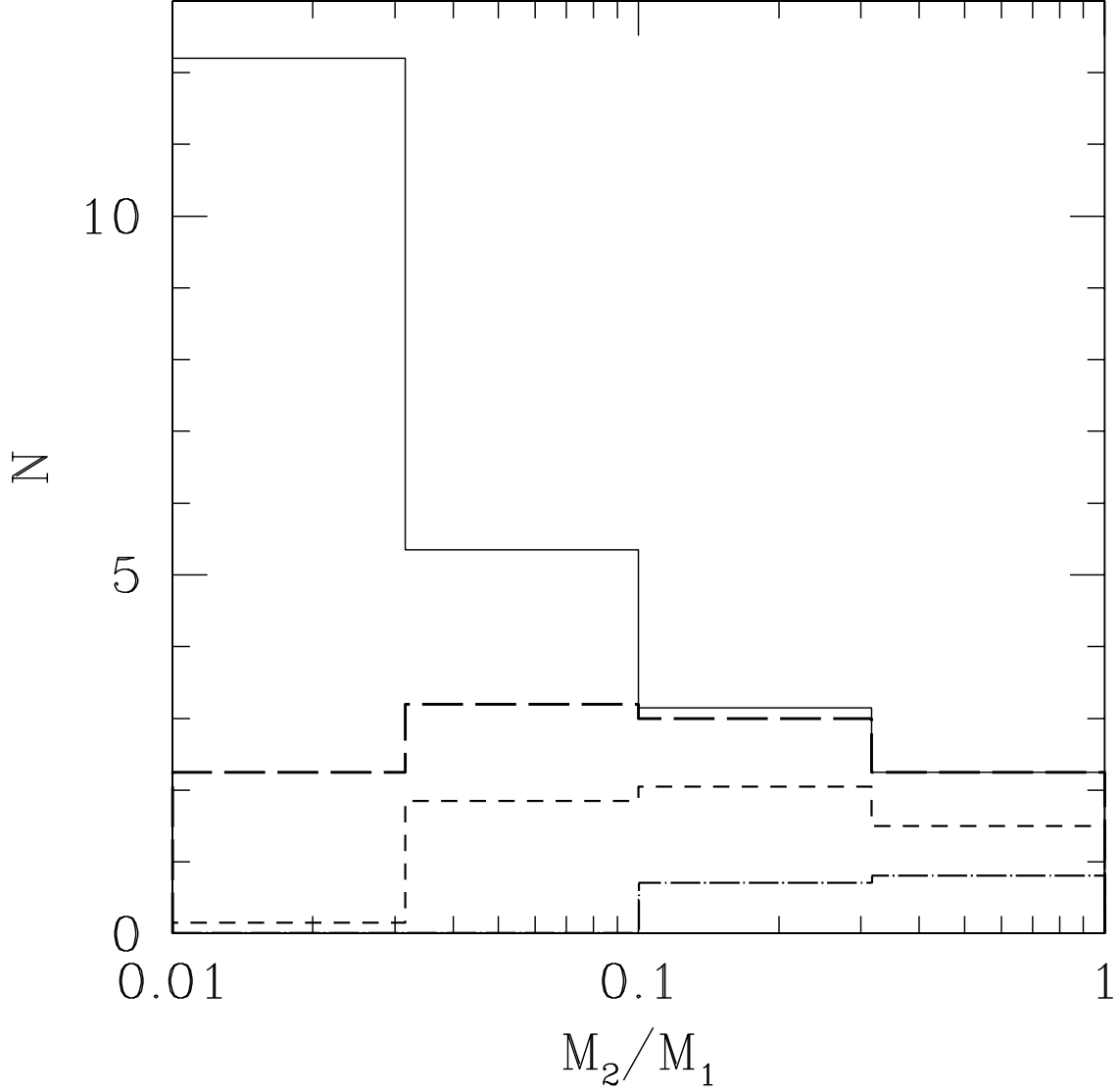


Fig. 7.— Number of mergers per logarithmic secondary-to-primary mass ratio, extracted from the merger history of a $M_0 = 10^{13} M_\odot$ halo at $z = 0$, and averaged over 20 merger trees. The total number of mergers experienced by the halo at $z < 3$ is shown by the solid histogram. $z < 3$. The number of *efficient* mergers (see the text for the definition) experienced by the same halo at different redshift is shown by the long-dashed (for $z < 3$), short-dashed (for $z < 2$), and dot-dashed (for $z < 1$) histograms.